Available online at www.sciencedirect.com
ScienceDirect
Journal of Power Sources 174 (2007) 867–871
JOURNAL OF POWER SOURCES
www.elsevier.com/locate/jpowsour

Short communication

Electrochemical and structural studies of the carbon-coated $Li[Cr_xLi_{(1/3-x/3)}Ti_{(2/3-2x/3)}]O_2$ ($x = 0.3, 0.35, 0.4, 0.45$)

Xin Mi, Hong Li, Xuejie Huang *

Beijing National Laboratory for Condensed Matter Physics, Institute of Physics, Chinese Academy of Sciences, Beijing 100080, China

Available online 27 June 2007

Abstract

A series of carbon-coated layered structured $Li[Cr_xLi_{(1/3-x/3)}Ti_{(2/3-2x/3)}]O_2$ samples ($0.3 \le x \le 0.45$) were prepared. Among them, the sample of $x = 0.4$ shows the highest initial reversible capacity of 207 mAh g^{-1} at 30 mA g^{-1} in 2.5–4.4 V. The reversible Li-storage capacities for the samples with high x values ($x = 0.4, 0.45$) faded slightly while the samples with low Cr content ($x = 0.3$ and 0.35) showed a capacity increase upon cycling. It was found that the relative intensity ratio of (0 0 3) peak to (1 0 4) peak ($R_{(003)} = I_{(003)}/I_{(104)}$) is influenced strongly by x value in as-prepared samples. The samples of $x = 0.35$ and 0.4 turn to a similar structure with low $R_{(003)}$ value during cycling. These phenomena indicate that the cation mixing of Cr^{3+} in the lithium layer occurs in as-prepared samples and became more significant upon delithiation and lithiation. This is supposed being a necessary process for Cr-based layered structure materials possessing electrochemical reactivates. The occurrence of the cation mixing is beneficial from the local lattice distortion caused by the short-range ordering between Ti and Li. This is supposed to be helpful for the migration of Cr^{6+} and Cr^{3+} at tetrahedral and octahedral sites. Different from the case of $LiNiO_2$, the cation mixing is essential for the transport and storage of lithium in the carbon-coated Li–Cr–Ti–O layered compounds.

Keywords: Li–Cr–Ti–O; Li-ion batteries; Local lattice distortion; Carbon coating

1. Introduction

Cr-based layered structured cathode materials [1–8] attract much attention due to their unique one step three-electron charge transfer feature. A reversible capacity of 173 mAh g^{-1} (2.5–4.4 V, 7.5 mA g^{-1} rate) was obtained in layered structured $Li[Li_{0.2}Cr_{0.4}Mn_{0.4}]O_2$ compound [4], while optimized Li–Cr–Ti–O compound delivered a discharge capacity of 203 mAh g^{-1} at 60 °C were also reported [7,8]. In order to overcome their shortage of low rate capability performance at room temperature, we found recently that $Li[Li_{0.2}Cr_{0.4}Ti_{0.4}]O_2$ particles could be coated with a layer of carbon. Layered structure was maintained and no impurities were introduced [9]. As similar as in the case of insulating $LiFePO_4$ [10–12], it is demonstrated that the carbon coating on $Li[Li_{0.2}Cr_{0.4}Ti_{0.4}]O_2$ is a very effective way to improve its capacity and the rate performance. The carbon-coated $Li[Li_{0.2}Cr_{0.4}Ti_{0.4}]O_2$ shows much enhanced capacity (207 mAh g^{-1}, 0.2 C, 2.5–4.4 V) and rate performance (154 mAh g^{-1}, 1 C, 2.5–4.4 V) due to the improvement of electronic contact.

The structure evolution of Li–Cr–Mn–O layered compounds in the charge/discharge process was intensively investigated by XRD and XAS [4–6]. It was shown the Cr migration during cycling. A similar result in Li–Cr–Ti–O compounds was also reported by Zhang and Noguchi [7,8].

However, the effects of Ti and Li in the transition metal/lithium layer on the capacity and the relationships among composition, structure and electrochemical behaviors are yet to be understood.

In this paper, carbon-coated $Li[Cr_xLi_{(1/3-x/3)}Ti_{(2/3-2x/3)}]O_2$ samples with $x = 0.3, 0.35, 0.4, 0.45$ were compared. The unusual electrochemical behaviors of the Cr-based layered compounds are revealed and explained primarily based on the structure information.

2. Experimental

$Li[Cr_xLi_{(1/3-x/3)}Ti_{(2/3-2x/3)}]O_2$ ($x = 0.3$, 0.35, 0.4, 0.45) compounds were prepared by a "sol–gel" method. Stoichiometric amounts of $CH_3CO_2Li{\cdot}2H_2O$, $Cr(NO_3)_3{\cdot}9H_2O$ and $Ti(OC_4H_9)_4$ (99.0%, Beijing reagent) were dissolved in CH_3CH_2OH in a beaker. $NH_3{\cdot}H_2O$ was dropped into the solution to form a gel after a few hours. Then the beaker was heated

* Corresponding author.
E-mail address: xjhuang@aphy.iphy.ac.cn (X. Huang).

0378-7753/$ – see front matter © 2007 Elsevier B.V. All rights reserved.
doi:10.1016/j.jpowsour.2007.06.104

in an oven at 80 °C to remove the solvent. The precipitate was ground for 30 min and then heated in a tube furnace at 800 °C for 24 h under flowing argon, and cooled in the furnace to get the final products. Carbon-coated $Li[Cr_xLi_{(1/3-x/3)}Ti_{(2/3-2x/3)}]O_2$ samples were prepared by mechanically mixing the pristine Li–Cr–Ti–O powder with sugar at a weight percent of 1:1 for 2 h and then pyrolyzing in a tube-furnace at 600 °C for 10 h under flowing argon. The carbon content in the final composite was estimated to be 15 wt% from the amount of metals in the samples obtained by ICP analysis. The nominal and the obtained compositions of the pristine compounds were given as following.

$x = 0.3$:	$Li_{1.233}Cr_{0.3}Ti_{0.467}O_2$	$Li_{1.226}Cr_{0.304}Ti_{0.470}O_2$
$x = 0.35$:	$Li_{1.217}Cr_{0.35}Ti_{0.433}O_2$	$Li_{1.208}Cr_{0.355}Ti_{0.437}O_2$
$x = 0.4$:	$Li_{1.2}Cr_{0.4}Ti_{0.4}O_2$	$Li_{1.189}Cr_{0.407}Ti_{0.404}O_2$
$x = 0.45$:	$Li_{1.183}Cr_{0.45}Ti_{0.367}O_2$	$Li_{1.176}Cr_{0.455}Ti_{0.369}O_2$

X-ray diffraction (XRD) was performed on a Panalytical X'pert Pro MPD diffractometer using Cu Kα radiation. Cell parameters were obtained using dicvol91 software [13]. The X-ray photoelectron spectroscopy analysis was performed on a PHI Quantera SXM using an Al X-ray source and the binding energies (BE) were determined with reference to the C1s signal. The cathode was composed of the composite (83 wt%), carbon black (10 wt%) and polyvinylidene fluoride (PVDF) binder (7 wt%). Aluminum foil was used as the current collector. A lithium metal foil was used as the counter electrode and reference electrode. The electrolyte was 1 M $LiPF_6$ in ethylene carbonate and dimethyl carbonate solution (EC + DMC, 1:1 in volume). All the cells were cycled with a Land battery test instrument at room temperature. For the *ex situ* XRD experiments, titanium foil was used as the current collector and the cells were charged and discharged at 150 mA g^{-1} current density to the preset voltage. For the *ex situ* XPS experiments, the cells were charged and discharged at 30 mA g^{-1} current density to the preset voltages. The cathodes were taken out in the glove box and rinsed with anhydrous dimethyl carbonate then stored in a dry sealed container until XRD or XPS measurements.

3. Results and discussion

Fig. 1 shows the X-ray diffraction patterns of the carbon-coated $Li[Cr_xLi_{(1/3-x/3)}Ti_{(2/3-2x/3)}]O_2$ samples ($x = 0.3$, 0.35, 0.4, 0.45). All the diffraction peaks of the samples were indexed on the rhombohedra α-$NaFeO_2$ structure (*R*-3*m* space group, No. 166). No peaks of carbon can be observed, implying that the coating-layer of carbon is amorphous. The splitting of (0 1 8) and (1 1 0) can be distinguished in the samples with $x = 0.3$, 0.35 and 0.45 except $x = 0.4$. The later shows a much broaden pattern than the others, indicating a small grain size. Therefore, the (0 1 8) and (1 1 0) peak may be overlapped in this sample.

$Li[Cr_xLi_{(1/3-x/3)}Ti_{(2/3-2x/3)}]O_2$ consists of lithium layer (3b sites) alternating with transition metal/lithium layer (3a sites), separated by oxygen layer (6c sites). $[Cr_xLi_{(1/3-x/3)}Ti_{(2/3-2x/3)}]$ represents the transition metal/lithium layer. In Fig. 1, a peak appears in the region of 21°, marked by the arrows, which could

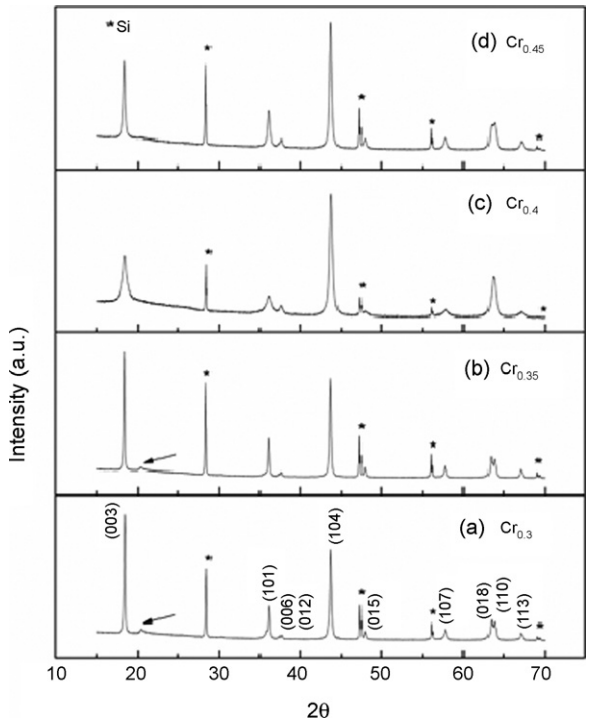

Fig. 1. XRD patterns of the carbon-coated $Li[Cr_xLi_{(1/3-x/3)}Ti_{(2/3-2x/3)}]O_2$: (a) $x = 0.3$, (b) $x = 0.35$, (c) $x = 0.4$, and (d) $x = 0.45$.

be regarded as short-range ordering between Ti and Li. Similar results can be observed in the Li–Cr–Mn–O materials [3,4]. Experiment analysis showed that there are local domains of Cr- and Mn-rich regions in the transition metal/lithium layer of the material and the lithium ions appear to be clustered preferentially around Mn. Local short-range ordering between Ti and Li or Mn and Li can be understood in terms of Pauling's rule of electroneutrality [4,14]. In layered phases, only $LiM^{3+}O_2$ and $Li[M^+_{1/3}M^{4+}_{2/3}]O_2$ stoichiometries can preserve local electroneutrality around oxygen. In Fig. 1, it can be observed that the peak intensity around 21° decreases along with the increased Cr content in the samples. This can be explained by assuming that the extent of the local short-range ordering between Ti and Li decreases when the content of Cr increases in the transition metal/lithium layer.

As the cell parameters with error bars of the samples illustrated in Fig. 2, there is no evident change in *a* axis or *c* axis. It is noted that the strongest peak in the XRD patterns of the samples of $x = 0.4$ and 0.45 is (1 0 4) while the strongest peak is (0 0 3) in those of the low Cr content samples, which will be discussed later.

Fig. 3 shows the charge–discharge voltage curves of the carbon-coated $Li[Cr_xLi_{(1/3-x/3)}Ti_{(2/3-2x/3)}]O_2$ at 0.2 C (30 mA g^{-1} current density) between 2.5 and 4.4 V. The voltage profiles for all the samples are very similar. A large irreversible capacity in the first cycle was observed in all samples, similar to the results of Li–Cr–Mn–O materials [1–6]. It is noted that the discharge capacity at the second cycle for the low Cr content samples increased relative to that of the first cycle, while the capacity of the high Cr content samples decreased upon cycling. As shown in Table 1, the sample of x = 0.4 delivered the highest

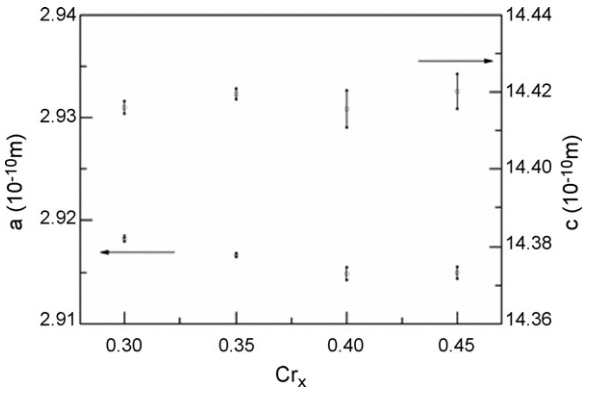

Fig. 2. Cell lattice parameters in the carbon-coated $Li[Cr_xLi_{(1/3-x/3)}Ti_{(2/3-2x/3)}]O_2$.

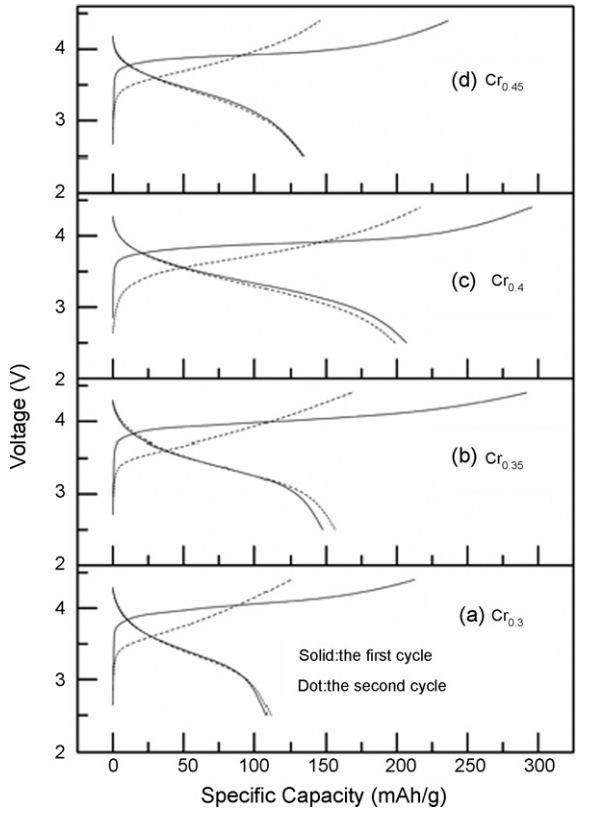

Fig. 3. Charge–discharge voltage curves of the carbon-coated $Li[Cr_xLi_{(1/3-x/3)}Ti_{(2/3-2x/3)}]O_2$ at 30 mA g^{-1} current density in the range of 2.5 and 4.4 V: (a)–(d) as in Fig. 1.

Table 1
Charge, discharge and irreversible capacities for all the samples for the first cycle between 2.5 and 4.4 V at the rate of 30 mA g^{-1} current

Sample	Charge capacity (mAh g^{-1})	Discharge capacity (mAh g^{-1})	Irreversible capacity (mAh g^{-1})
$X=0.3$	213	108	105
$X=0.35$	292	148	144
$X=0.4$	296	207	89
$X=0.45$	236	134	102

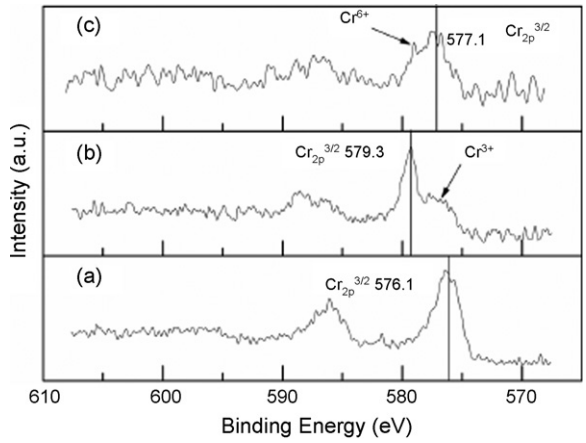

Fig. 4. XPS patterns for Cr in pristine $Li_{1.2}Cr_{0.4}Ti_{0.4}O_2$: (a) fresh material, (b) charged to 4.4 V (30 mA g^{-1} current density), and (c) charged to 4.4 V then discharged to 2.5 V (30 mA g^{-1} current density).

charge and discharge capacities of 296 and 207 mAh g^{-1} for the first cycle, respectively.

In order to investigate the charge transfer mechanism in the charge–discharge process, the XPS analysis was performed on the $Li_{1.2}Cr_{0.4}Ti_{0.4}O_2$ without carbon coating to avoid the interference from carbon. The XPS patterns for pristine $Li_{1.2}Cr_{0.4}Ti_{0.4}O_2$ are shown in Figs. 4(a) and 5(a). Cr and Ti are in the valence state of +3 and +4. The XPS results of the charged and discharged state are shown in Figs. 4(b and c) and 5(b and c). It can be seen clearly that the Cr(III) ions are oxidized into Cr(VI) ions during delithiation and vice verse during lithiation while Ti ions do not participate in the charge transfer in the full charge–discharge process.

It is known that Cr^{3+} cation has high stabilization energy for the octahedral sites and Cr^{6+} cation prefers to stay in the tetrahedral sites. In the first charge process, Cr^{3+} cations are oxidized into Cr^{6+} cations and move to the tetrahedral sites out of the transition metal/lithium layer, accompanying with the shrink of the *c* axis. Such a motion is not possible in the case of $LiCrO_2$ due to the structure limitation. However, the short-range ordering between Ti and Li in Cr^{3+} layer occurs in $Li[Cr_xLi_{(1/3-x/3)}Ti_{(2/3-2x/3)}]O_2$ and leads to a local lattice dis-

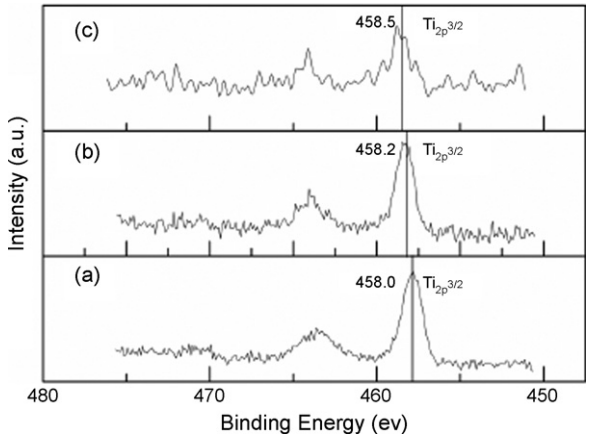

Fig. 5. XPS patterns for Ti in pristine $Li_{1.2}Cr_{0.4}Ti_{0.4}O_2$: (a)–(c) as in Fig. 4.

tortion. This is supposed to be beneficial for the Cr migration. In the lithium re-intercalation process, Cr^{6+} is converted to Cr^{3+}, while it may move to the octahedral sites either in the transition metal/lithium layer or in the lithium layer. The occupation of Cr^{3+} at the sites in the lithium layer is an irreversible process and results in the large irreversible capacity at first cycle. This was evidenced by the fact that $I_{(003)}/I_{(104)}$ of $Li_{1.2}Cr_{0.4}Ti_{0.4}O_2$ is decreased after the first lithium extraction in our previous result [9] and in new result shown later. According to Fig. 3, $Li_{1.2}Cr_{0.4}Ti_{0.4}O_2$ seems to be an optimized composition with equal content of Ti and Cr. When the content of Cr is too high, less local lattice distortion hinders the migration of Cr out of the layer of transition metal/lithium layer, which should be also the reason of inactivity of $LiCrO_2$ as mentioned above.

The cycling performance of the carbon-coated $Li[Cr_xLi_{(1/3-x/3)}Ti_{(2/3-2x/3)}]O_2$ at different current densities between 2.5 and 4.4 V is illustrated in Fig. 6. It can be observed that the cyclic performance is quite good for all the samples and at all the rates, while the sample of $x = 0.4$ appear to have better rate performance. It hints also that local lattice distortion resulted by short range Ti–Li ordering is also beneficial for kinetics. Furthermore, it is obvious that for the low Cr content samples, there is a distinct capacity increase during the first 20 cycles before it reaches a stable value. In addition, the higher the rate is, the more distinct the capacity increase is. It implies that a slow activation process exist upon cycling. At the same rate for the samples of $x = 0.35$ and 0.4, in spite of the initial capacity difference, the discharge capacities are almost the same after 50 cycles. The

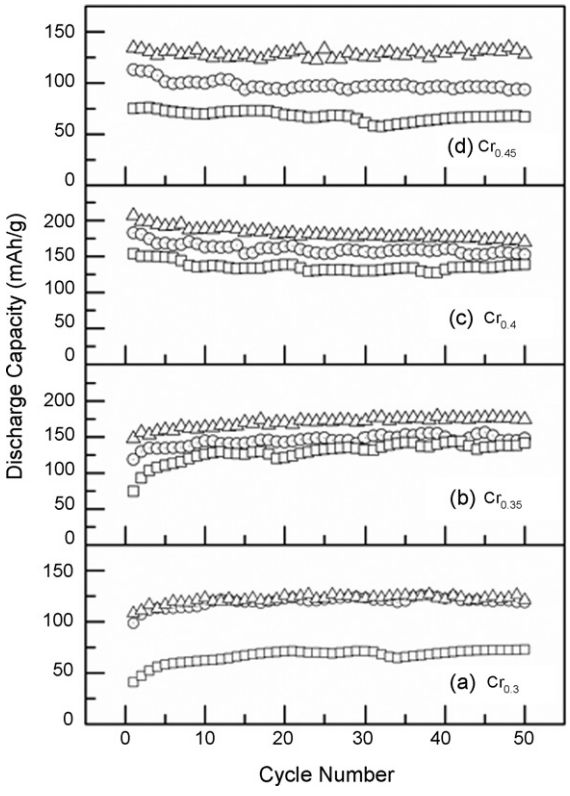

Fig. 6. The cycling performance of the carbon-coated $Li[Cr_xLi_{(1/3-x/3)}Ti_{(2/3-2x/3)}]O_2$ at different current densities in the range of 2.5 and 4.4 V: (a)–(d) as in Fig. 1; (□) 150 mAh g^{-1}, (◯) 75 mA g^{-1}, (△) 30 mA g^{-1}.

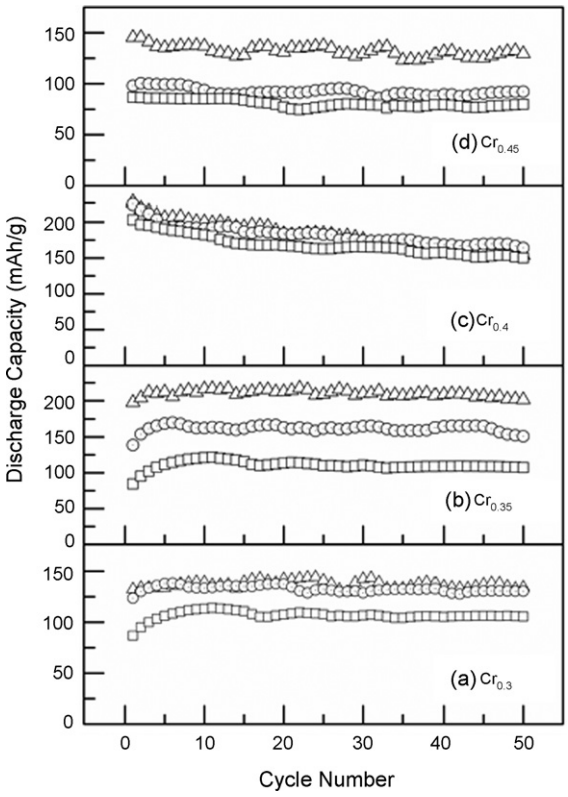

Fig. 7. The cycling performance of the carbon-coated $Li[Cr_xLi_{(1/3-x/3)}Ti_{(2/3-2x/3)}]O_2$ at different current densities in the range of 2.0 and 4.8 V: (a)–(d) as in Fig. 1; (□) 300 mAh g^{-1}, (◯) 150 mA g^{-1}, (△) 75 mA g^{-1}.

samples of $x = 0.35$ and 0.4 showed the discharge capacities of 174 and 170 mAh g^{-1} at 0.2 C (30 mA g^{-1} current density) and those of 142 mAh g^{-1} and 139 mAh g^{-1} at 1 C (150 mA g^{-1} current density) at the 50th cycle, respectively.

It is found that in a wide voltage range between 2.0 and 4.8 V, the cyclic performance is still good for all the samples and at all the rates, as shown in Fig. 7. Activation process for the low Cr content samples can also be seen. The rate performance of the sample of $x = 0.35$ is not as good as that of the sample of $x = 0.4$, however, it shows a perfect cyclic performance at 0.5 C (75 mA g^{-1} current density) and delivers a discharge capacity of 201 mAh g^{-1} at the 50th cycle. It may be imagined that certain level of local distortion in the transition metal/lithium layer is beneficial for kinetics.

As shown in Fig. 8, *ex situ* XRD study was performed to investigate the structure change of the carbon-coated $Li[Cr_xLi_{(1/3-x/3)}Ti_{(2/3-2x/3)}]O_2$ materials during cycling. It can be observed that for both the samples of $x = 0.35$ and 0.4 the layered structure is maintained although there are obvious changes occurred after 30 cycles such as peak width and (0 0 3) peak intensity. It is noted that the diffraction patterns of the samples of $x = 0.35$ and 0.4 are almost the same after 30 cycles although they are obviously different before cycling.

In the layered structured compounds [15–18], $R_{(003)} = I_{(003)}/I_{(104)}$ can be used as an indicator for cation mixing. The lower value means a high degree of cation mixing, due to the occupancy of the transition metal in the lithium layer. In our case, $R_{(003)}$ of the samples of $x = 0.35$ and 0.4 is 1.04 and 0.36

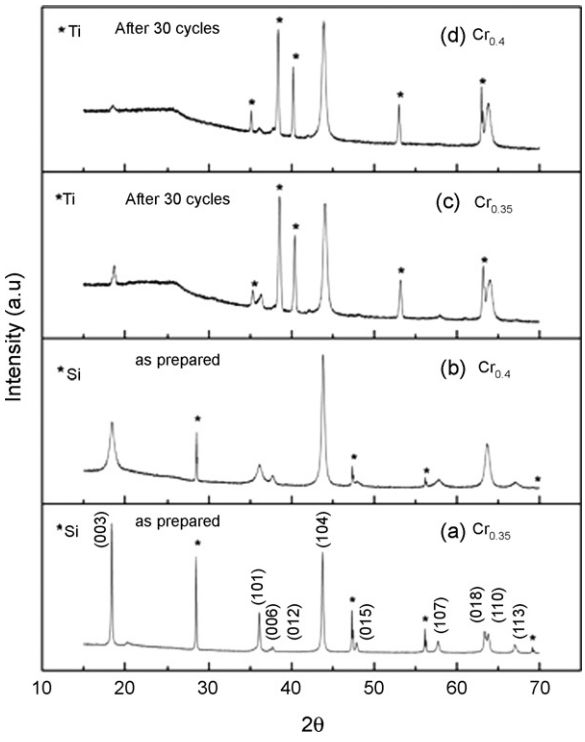

Fig. 8. XRD patterns of the carbon-coated $Li[Cr_xLi_{(1/3-x/3)}Ti_{(2/3-2x/3)}]O_2$: (a) $x = 0.35$, as prepared, (b) $x = 0.35$, after 30 cycles at 150 mA g^{-1} current density in the range of 2.0–4.8 V, (c) $x = 0.4$, as prepared, and (d) $x = 0.4$, after 30 cycles at 150 mA g^{-1} current density in the range of 2.0–4.8 V.

before cycling while that changes to 0.17 and 0.05 accordingly after 30 cycles. $R_{(0\,0\,3)}$ decreases for both the samples, however, the change in that of the sample of $x = 0.35$ is much more evident, indicating more significant structural changes.

As we discussed above, local lattice distortion seems essential for Cr^{6+} migration and Li-extraction, which is related to the existence of Ti–Li short-range ordering in the transition metal/lithium layer. It can be seen from Fig. 1, $Li_{1.2}Cr_{0.4}Ti_{0.4}O_2$ shows the more significant mixing occupation in as-prepared sample. This may explain that it shows the highest electrochemical reactivity and its activation process is less evident in $Li[Cr_xLi_{(1/3-x/3)}Ti_{(2/3-2x/3)}]O_2$.

During cycling, the crystalline structures of the samples of $x = 0.35$ and 0.4 turn to a more "similar" and "steady" one in which $R_{(0\,0\,3)}$ decreases further for both the samples. This indicates further that the cation mixing structure is beneficial for the transport and storage of lithium for Cr-based layered structure compounds, which is much different from the case of $LiNiO_2$.

4. Conclusions

$Li[Cr_{0.4}Li_{0.2}Ti_{0.4}]O_2$ shows the highest charge and discharge capacities in the series of $Li[Cr_xLi_{(1/3-x/3)}Ti_{(2/3-2x/3)}]O_2$. It delivered a discharge capacity of 207 mAh g^{-1} at 0.2 C between 2.5 and 4.4 V for the first cycle. The reversible Li-storage capacities for the samples with high x values ($x = 0.4$, 0.45) faded slightly while the samples with low Cr content ($x = 0.3$ and 0.35) showed a capacity increase upon cycling. XRD investigation revealed that the sample of $Li[Cr_{0.4}Li_{0.2}Ti_{0.4}]O_2$ shows the most significant cation mixing. During cycling, the crystalline structures of the samples of $x = 0.35$ and 0.4 as investigated turn to low $R_{(0\,0\,3)}$ value. These phenomena indicates that the cation mixing is an important approach to improve the capacity and rate capability of Cr-based layered structured cathode materials. The content of cation mixing is related to the local lattice distortion caused by the short-range ordering between Ti and Li in the transition metal/lithium layer, which is supposed to help the Cr^{6+} migration upon delithiation. The investigation on fine structural variation is needed for further clarification on this relationship between structural feature and electrochemical performances.

Acknowledgement

Financial supports from National "863" Projects (Contract No. 20060103Z2028).

References

[1] C. Storey, I. Kargina, Y. Grincourt, I.J. Davidson, Y.C. Yoo, D.Y. Seung, J. Power Sources 97–98 (2001) 541.
[2] Y. Grincourt, C. Storey, I.J. Davidson, J. Power Sources 97–98 (2001) 711.
[3] M. Balasubramanian, J. McBreen, I.J. Davidson, P.S. Whitfield, I. Kargina, J. Electrochem. Soc. 149 (2002) A176.
[4] B. Ammundsen, J. Paulsen, I.J. Davidson, R.S. Liu, C.H. Shen, J.M. Chen, L.Y. Jang, J.F. Lee, J. Electrochem. Soc. 149 (2002) A431.
[5] Z.H. Lu, J.R. Dahn, J. Electrochem. Soc. 149 (2002) A1454.
[6] Z.H. Lu, J.R. Dahn, J. Electrochem. Soc. 150 (2003) A1044.
[7] L.Q. Zhang, H. Noguchi, Electrochem. Commun. 4 (2002) 560.
[8] L.Q. Zhang, H. Noguchi, J. Electrochem. Soc. 150 (2003) A601.
[9] X. Mi, H. Li, X.J. Huang, Electrochem. Solid-State Lett. 9 (7) (2006) A324.
[10] N. Ravet, Y. Chouinard, J.F. Magnan, S. Besner, M. Gauthier, M. Armand, J. Power Sources 97–98 (2001) 503.
[11] M.M. Doeff, Y. Hu, F. Mclarnon, R. Kostecki, Electrochem. Solid-State Lett. 6 (10) (2003) A207.
[12] H. Huang, S.C. Yin, L.F. Nazar, Electrochem. Solid-State Lett. 4 (10) (2001) A170.
[13] A. Boultif, D. Louer, J. Appl. Crystallogr. 24 (1991) 987.
[14] G.C. Mather, C. Dussarrat, J. Etourneau, A.R. West, J. Mater. Chem. 10 (2000) 2219.
[15] J. Morales, C. Perez-Vicente, J.L. Tirado, Mater. Res. Bull. 25 (1990) 623.
[16] T. Ohzuku, A. Ueda, M. Nagayama, Y. lwakoshi, H. Komori, Electrochim. Acta 38 (1993) 1159.
[17] E.D. Jeong, M.S. Won, Y.B. Shim, J. Power Sources 70 (1998) 70.
[18] M. Song, I. Kwon, H. Kim, J. Appl. Electrochem. 35 (2005) 1073.